AN INVESTIGATION ON THE CORROSION RESSISTANCE OF THE CALCIUM MAGNESIUM ALUMINATE CEMENT BONDED ALUMINA-SPINEL REFRACTORY CASTABLES

Xingwu Tan[1], Nan Li[1], Wen Yan[1], Bingqiang Han[1]

The State Key Laboratory of Refractories and Metallurgy, Wuhan University of Science and Technology, Wuhan, China

13501074107@163.com.

ABSTRACT

Four types of Al_2O_3-spinel castables (total spinel containing 20%) with alternative binders CMA or CA and with or without microsilica (0 or 1%) were prepared. In order to evaluate the influence of the microstructure evolution on the corrosion behavior, the static crucible test considering a basic slag (CaO/SiO_2=2.0 wt%) as a reactant via SEM/EDS analysis and the thermo-chemical simulation via FactSage® software were carried out respectively. The corrosion results revealed that the CMA bonded castables firing at 1600 ℃ before slag attack induced a fine texture in the matrix, which played an important role in improving corrosion resistance. The addition of microsilica will affect the morphology and the location of the generated CA_6, which further affected the corrosion resistance. For the castable without microsilica, CA_6 layer was found at the border of the aggregates, protected aggregates from slag attack, while with microsilica, CA_6 was mainly formed in the matrix, resulted in the aggregates unprotected and dissolved rapidly. The phase evolution of corroded samples was in tune with the simulation analysis.

Keywords: Corrosion; Spinel; Castable; Cement; Microstructure; Thermo-chemical simulation

INTRODUCTION

The calcium aluminate cement (CA) bonded Al_2O_3-spinel castable (preformed spinel containing) has been used as steel ladle lining for decades years due to the outstanding performances. Nevertheless, considering the various size of spinel, the castables containing preformed spinel presents less efficient on the corrosion resistance compared to the Al_2O_3-MgO castable containing in situ spinel [1, 2].

In recent year, novel calcium magnesium aluminate cement (CMA) has been developed, with the distinct microstructure of calcium aluminate phases embedded in a matrix of microcrystalline spinel (~3μm) [3, 4]. The CMA bonded castables presented lower apparent porosity, smaller median micropore size and the well distributed microcrystalline spinel in the matrix. As a result, the CMA bonded castables presented higher corrosion resistance than the CA bonded ones [3, 4]. Nevertheless, the relevant investigation about the influence of the microstructure evolution on the corrosion behavior needed further study. Considering this aspect, the purpose of the work was to examine the slag-refractory interface of corroded castables via the SEM/EDS analysis accompanied by the thermo-chemical simulation to get more understanding of this relationship.

EXPERIMENTAL

Four model castable formulations using alternative binders (CMA or CA) with different microsilica content (0 or 1%) were prepared (as shown in Tab.1). The castables comprised 70wt% of tabular alumina aggregate (6-0.2mm) and 30% of the matrix including reactive alumina, preformed spinel (~45μm, 73% Al_2O_3), CMA or CA cement, microsilica etc. The chemical composition of the CMA binder (containing 70% of microcrystalline spinel) was 70% Al_2O_3, 20% MgO and 10% CaO; while the CA binder was 70% Al_2O_3 and 30% CaO. In general, the model castables were designed containing 20 wt% of spinel (or 5% of MgO) and 1.5% of CaO. The chemical composition of the model castables and the basic slag for corrosion test were listed in Tab.2. The experimental procedure was described as follows:

At first, the simulations were carried out using the FactSage® thermo-chemical software (version 6.2). In order to evaluate the influence of the overall composition of the castables on the corrosion behavior, the thermodynamic calculation modeling proposed by Berjonneau et al. [5] was used, considering the reaction of all possible proportions (in mass) between slag-refractory as a function of the reaction rate <A> at 1600 ℃. <A> was defined by ratio: (R)/[(S)+(R)] with(S)+(R)=1 (R is the refractory and S the slag). The predicted phase evolutions as a function of <A> were carried out. Next, the samples were vibrated with the required water for processing. The rectangular samples (160mm×40mm×40mm) and the crucibles (with an external top 100/bottom 90mm diameter, 100mm height and with an internal hole of 50/45mm diameter and 60mm depth)

were prepared. After cured at 20 ℃ for 24h and dried at 110 ℃ for 24h, the samples were fired at 1600 ℃ for 2h in an electric chamber furnace. Then, the rectangular samples were used for physical property test, subsequently, the crucibles incorporated with 80 g of the slag powder, were fired at 1600 ℃ for 1 hour for corrosion test.

Tab.1 Formulations of the model refractory castables

Raw materials (wt %)	A0	A1	M0	M1
Tabular alumina	70	70	70	70
Reactive alumina	5	4	5	4
Preformed spinel	20	20	10	10
CMA binder	-	-	15	15
CA binder	5	5	-	-
Microsilica	-	1	-	1
Polycarboxylate ether	0.1	0.1	0.1	0.1
Water addition	5.0	5.0	5.0	5.0

Tab.2 Chemical composition of the castables and slag (wt %)

	Al_2O_3	SiO_2	MgO	CaO	Fe_2O_3	MnO
A0 (M0)	93.5	-	5	1.5	-	-
A1 (M1)	92.5	1	5	1.5	-	-
slag	9.7	19.9	5.0	40.2	22.2	3.0

After that, the apparent porosity was evaluated using the Archimedes technique in water. Based on the SEM micrographs of the polished samples, the median pore size in the matrix (<200μm) were measured using image analysis method. Then, the corrosion indexes I_c were determined by inspecting the cross-section area of the corroded samples by counting pixels method, where $I_c=S_c/S_o \times 100\%$, S_o was the original section area of the internal hole, S_c was the section area of refractory completely corroded by slag. Finally, the polished section area at the interface (~15mm width and length) took from the bottom of the hole was analyzed. The chemical composition in the matrix and the phase evolution at the interface from slag to refractory were identified by scanning electron microscope (SEM, EVO18, ZEISS, Germany) equipped with energy dispersive X-ray spectroscope (EDS, INCA X-Max50, Oxford, UK). The chemical composition was analyzed statistically in the area within 1mm depth of a step of 1mm, based on which the liquid content was carried out using the FactSage® software.

RESULTS AND DISCUSSION

The thermo-chemical simulation at 1600 ℃ was carried out. The predicted phase evolutions for corroded castables (at 1600 ℃) as function of <A> were plotted in Fig.1.

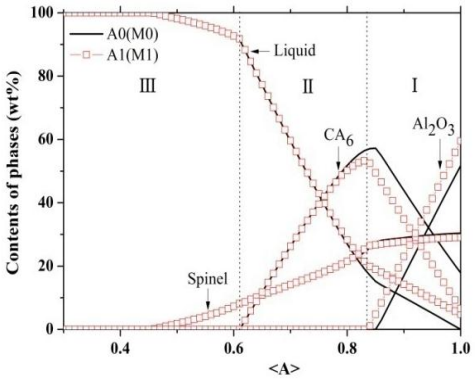

Fig.1 The predicted phase evolutions as a function of <A>

Because of the chemical composition similarities between castables A0 (M0) and A1 (M1), the predicted phases between the castables were qualitatively similar and the same sequence. Regarding the A0 model as a reference, the phase evolutions as a function of <A> could be divided into three zones according to the solid and liquid amount. In the first zone, as slag reacted with the refractories, the solid phase Al_2O_3 dissolved in the slag accompanied by the reaction of Al_2O_3(l) with CaO(l) resulting in the CA_6 precipitation[6]. The CA_6 content reached to the maximum when Al_2O_3 was completely dissolved. During this time, spinel content decreased slowly and the liquid amount increased slightly (from 0 to 15%). In the second zone, as <A> decreased further, CA_6 decreased from the maximum value to zero, the spinel content decreased slightly higher and the liquid amount rise significantly (from 15 to over 90 %). In the third zone, the solid spinel decreased and disappeared until the liquid phase left.

Despite composition similarities between A0 (M0) and A1 (M1), some differences were observed: For A0 (M0) without microsilica, the initial liquid content was zero, resulting in the CA_6 formation in the reaction of solid mechanism, while for A1 (M1) with microsilica, the initial liquid content was 5wt%, resulting in the CA_6 formation in the reaction of liquid mechanism. This led to the difference in morphology and location of the CA_6 generated in castables, which would drastically affect the castables' performance [6, 7].

Besides the chemical aspect, the apparent porosity and the micro pore size also affected the corrosion behavior. The SEM micrographs of fired sample matrix were shown in Fig.2. The corroded sample profiles were presented in Fig.3. According to the experimental procedure described above, the apparent porosity, the median pore size and the corrosion indexes were summarized in Tab.3. As shown in Tab.3, castable A0 and A1

presented higher apparent porosity and higher median pore size thanM0 and M1, which may be related to the microstructure of the castable. Additionally, compared to the apparent porosity, the median pore size was more closely related to the corrosion index. The castable A1 with the highest median pore size showed the highest slag corrosion index; while castable M0 with the lowest median pore size showed the lowest slag corrosion index. Castable A0 and M1 presented the intermediate profile between A1 and M0.

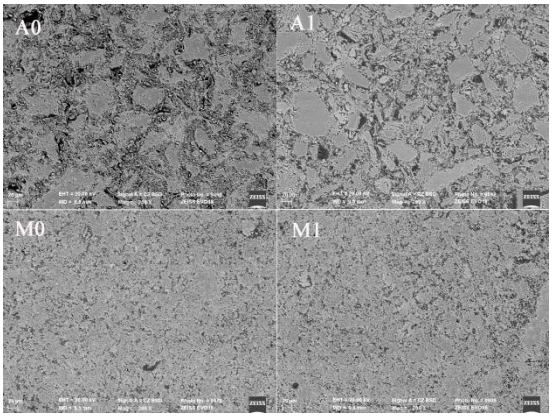

Fig.2 SEM micrographs of sample matrixes fired at 1600 ℃

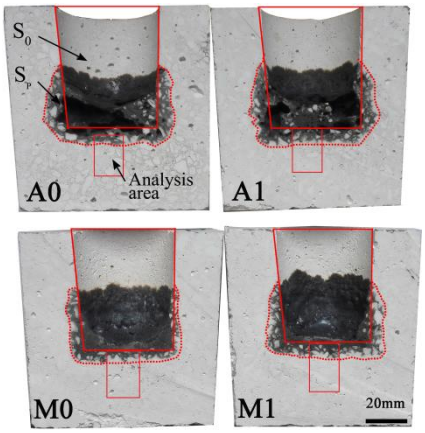

Fig.3 Corrosion profiles of model castables (the red regions at bottom hole were for microstructure analysis by SEM/EDS)

Tab.3 Physical properties and corrosion index of samples

Samples	Apparent porosity (%)	Median pore size D_{50} (μm)	Corrosion index (%)
A0	17.7	6.8	18.2
A1	17.0	9.8	21.8
M0	15.7	3.4	5.5
M1	14.3	4.5	12.2

According to the studies[6, 7], for fired castable with microsilica in the reaction of liquid mechanism before slag attack, CA_6 generated in acicular shape in the matrix resulted in the expansion effect and the increase of median pore size, which may decrease the corrosion resistance.

The liquid content at the interface of the corroded matrixes as a function of depth were carried out and was shown in Fig.4. In tune with the simulation results, the liquid content could be divided roughly in three zones according to the liquid amount.

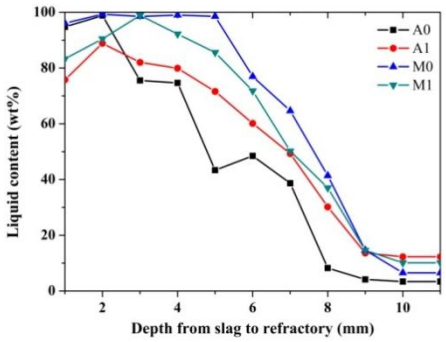

Fig.4 The liquid content in the matrix at the interface as a function of depth for different corroded castable

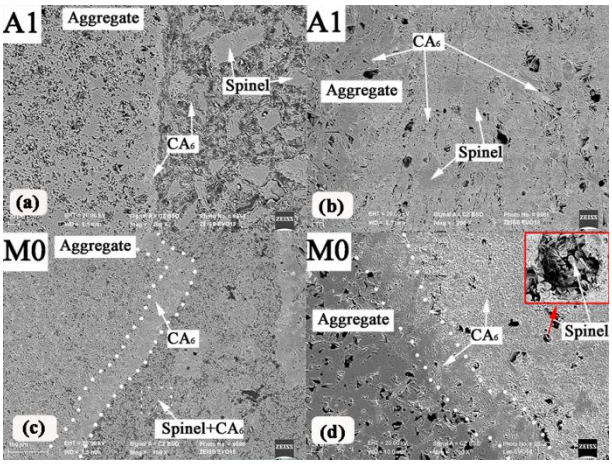

Fig.5 Typical SEM micrographs of the corroded castable ((a) A1: 9mm from hot face; (b) A1: 6mm from hot face; (c) M0: 9mm from hot face;; (d) M0: 6mm from hot face)

The typical castable A1 (presented the highest corrosion index) and M0 (presented the lowest corrosion index) were chosen to analyze as follows. For the castable A1: in the first zone (about 9-10mm from hot face), in the reaction of liquid mechanism, the acicular like CA_6 crystal mainly generated in the matrix. There was no well defined CA_6 layer formed at the border of the tabular alumina aggregates (as highlighting in Fig.5a) and the coarser preformed spinel was scattered in the matrix. In the second zone (about 3-9mm from hot face), due to the higher median pore size and the higher initial liquid content, which favored the slag infiltration, the liquid content increased significantly. The unprotected aggregates were quickly

consumed by the slag, followed by massive long platelet CA_6 (high aspect ratio) formation. As highlighting in Fig.5b, there was no noticeable border of aggregate any more, and further, Al_2O_3 in the inner tabular aggregate had completely reacted with the infiltrated slag, resulting in long platelet CA_6 forming in the inner aggregate. The CA_6 generated in the matrix with random orientation. The pore in the matrix was large and the pore amount was higher. All these features indicated that, the reaction took place in a non-uniform and quickly manner in the presence of liquid phase. A high amount of Fe and Mn ion was identified in the preformed spinel structure, indicating the role of spinel as Fe and Mn ion trapper. In the third zone (about 0-3mm from hot face), the liquid content reached to the highest value, and the main phase in the slag was identified as the glassy phase containing iron, and a mixture of CaO, Al_2O_3, SiO_2 and FeO_X which identified as gehlenite.

For the castable M0: in the first zone (about 9-10mm from hot face), the equiaxial CA_6 grain was identified both in the matrix and at the border of the aggregates. As the dotted line highlighting in Fig.5c, the CA_6 layer at the border of aggregates was fine and compact. The microcrystalline spinel (~3μm) embedded in the CA_6 grains in the matrix (the dotted square area highlighting in Fig.5c). Moreover, the median pore size was smallest among the castable. In the second zone (about 5-9mm from hot face), as highlighting in Fig.5d, the high density of CA_6 layer formed at the border and in the matrix (due to the lowest median pore size). The CA_6 generated in the matrix with fine orientation. Moreover, the pore in the matrix was smaller and the pore amount was lower. All these features indicated that, the reaction took place in a relatively more uniform and controlled manner. Besides that, the well distributed microcrystalline spinel incorporated with high amount of iron and manganese ions in the structure (shown in Fig.5d top right corner magnitude image) indicating the more efficient effect of fine spinel on trapping iron ion. In the third zone (about 0-5mm), the liquid reached to the highest amount, and the main phase was identified as glassy phase and gehlenite.

It should be noted that, despite of the castable A1 with no evident CA_6 layer formed at the border of aggregate and castable M0 with evident CA_6 layer formed at the border of aggregate, due to the physical property and the microstructure similarities, the corrosion behavior for castable A1 was close to A0, and M0 was close to M1.

Besides, it is highlighted that, the chemical compositions of Al_2O_3 in the remnant slag were different in the four crucibles, the rank of Al_2O_3 amount from low to high was: M0<M1<A0<A1, which also indicated the different wearing rate: M0<M1<A0<A1. This result was in tune with the rank of the corrosion index of castable: M0 < M1 < A0 < A1.

CONCLUSIONS

Based on the thermo-chemical simulation analysis and corrosion test results, the study reveals that, the CMA bonded castable presenting a fine microstructure with the smaller median pore size, the well distributed microcrystalline spinel in the matrix, which are responsible for the high corrosion resistance. The addition of microsilica will affect the morphology and the location of the generated CA_6, which may also have an effect on the corrosion resistance.

REFERENCES:

[1] S. Itose, M. Nakashima, T. Isobe, I. Shimizu, Improvement in the durability of alumina-spinel steel ladle castable containing spinel fine powder, Journal of the Technical Association of Refractories-Japan, 22[1] (2002):26-30.

[2]M. Sugawara, K. Asano, The recent developments of castable technology in Japan, In Proceedings of the Unified International Technical Conference on Refractories UNITECR'05, Orlando, USA, 30-34.

[3] Christoph Wöhrmeyer, Chris Parr, New spinel containing calcium aluminate cement for corrosion resistant castables aluminate technologies, Paris, France1-D-5.

[4] C. Wöhrmeyer, J. M. Aunray, Novel calcium magnesium aluminate bonded castables for steel and foundry ladles, In Proceedings of the Unified International Technical Conference on Refractories UNITECR'13, Victoria, Canada, 944-949.

[5] J Berjonneau, The development of a thermodynamic model for Al_2O_3-MgO refractory castable corrosion by secondary metallurgy steel ladle slag, Ceram. Int., 35[2] (2009):623-635.

[6] A.G. Tomba Martinez, A.P. Luz, M.A.L. Braulio, V.C. Pandolfelli, CA_6 impact on the corrosion behavior of cement-bonded spinel-containing refractory castables: An analysis based on thermodynamic simulations, Ceram. Int., 41 (2015):4714-4725.

[7] E.Y. Sako, In-depth microstructural evolution analyses of cement-bonded spinel refractory castables: novel insights regarding spinel and CA_6 formation, J. Am. Ceram. Soc., 5[95](2012):1732-1740.